



Published in final edited form as:

*Ophthalmology*. 2006 May ; 113(5): 792–9.e2.

## Corneal Pachymetry Mapping with High-speed Optical Coherence Tomography

Yan Li, MS<sup>1</sup>, Raj Shekhar, PhD<sup>2</sup>, and David Huang, MD, PhD<sup>3</sup>

<sup>1</sup> Department of Biomedical Engineering, Case Western Reserve University, Cleveland, Ohio.

<sup>2</sup> Department of Biomedical Engineering, Cleveland Clinic Foundation, Cleveland, Ohio.

<sup>3</sup> Cole Eye Institute, Cleveland Clinic Foundation, Cleveland, Ohio.

### Abstract

**Objective**—To map corneal thickness before and after LASIK with optical coherence tomography (OCT).

**Design**—Cross-sectional observational study.

**Participants**—Forty-two eyes of 21 normal subjects undergoing LASIK.

**Methods**—A high-speed (2000 axial scans/second) 1.3- $\mu\text{m}$ -wavelength corneal and anterior segment OCT prototype was used for corneal scanning. The scan pattern consisted of 10-mm radial lines on 8 meridians centered on the vertex reflection. The entire scan pattern of 1024 a-scans was acquired in 0.5 seconds. We developed automated computer processing for 3-dimensional corneal reconstruction and measurement. Corneal thickness was measured normal to the anterior surface and presented as color pachymetry maps and zonal statistics. The maps were divided into a central zone (<2 mm) and 3 annular areas (pericentral, 2–5 mm; transitional, 5–7 mm; peripheral, 7–10 mm), which were further divided into quadrantal zones. The average, minimum, and maximum corneal thicknesses were computed for zones within the 7-mm diameter. Optical coherence tomography and ultrasound pachymetry were measured 3 times at the preoperative and 3-month postoperative visits. Reproducibility was assessed by the pooled standard deviations (SDs) of the repeated measurements.

**Main Outcome Measures**—Optical coherence tomography pachymetric map and zonal statistic, and ultrasound pachymetry.

**Results**—Before LASIK, central corneal thicknesses (CCTs) were  $546.9 \pm 29.4 \mu\text{m}$  (mean  $\pm$  SD) for OCT and  $553.3 \pm 33.0 \mu\text{m}$  for ultrasound. After LASIK, CCTs were  $513.7 \pm 44.5 \mu\text{m}$  for OCT and  $498 \pm 46.6 \mu\text{m}$  for ultrasound. Optical coherence tomography and ultrasound CCT were highly correlated (Pearson correlation  $r = 0.97$  before LASIK and  $0.98$  afterwards). Optical coherence tomography CCT was slightly less than ultrasound CCT before surgery (mean difference,  $-6.4 \mu\text{m}$ ; 95% limits of agreement,  $-23.2$  to  $10.4 \mu\text{m}$ ) but slightly greater after LASIK ( $15.7 \mu\text{m}$ ;  $-1.6$  to  $33 \mu\text{m}$ ). These differences were statistically significant, but no more than the CCT measurement differences between ultrasound pachymeters. The reproducibility of the OCT zonal pachymetry averages was roughly  $2 \mu\text{m}$ .

**Conclusions**—High-speed OCT provided noncontact, rapid, reproducible pachymetric mapping over a wide area of the cornea. It is equivalent to ultrasound for CCT measurement before and after

---

Correspondence and reprint requests to David Huang, MD, PhD, Doheny Eye Institute, 1450 San Pablo Street, DEI 5702, Los Angeles, CA 99033. E-mail: dhuang@usc.edu.

Dr Huang has a patent royalty interest in optical coherence tomography technology. Drs Huang and Li receive research grant support from Carl Zeiss Meditec Inc. Dr Shekhar does not have a proprietary interest in the topic of the article.

Financial support: National Institutes of Health, Bethesda, Maryland (grant no.: R24 EY13015), and Carl Zeiss Meditec Inc., Dublin, California.

LASIK. This technology could be valuable for planning keratorefractive procedures and diagnosis of corneal diseases.

---

The measurement of corneal thickness (pachymetry) has important diagnostic and surgical applications. Central corneal thickness (CCT) is routinely used to monitor corneal edema and endothelial function,<sup>1-4</sup> manage ocular hypertension,<sup>5,6</sup> and plan common keratorefractive surgeries such as LASIK and photorefractive keratectomy (PRK).

Some pachymetry technologies provide only spot measurements, whereas others provide the capability to map a wide area of the cornea. Spot measurement technologies include traditional optical pachymetry,<sup>7</sup> specular and confocal microscopy,<sup>8</sup> ultrasound pachymetry,<sup>9,10</sup> and optical low-coherence reflectometry.<sup>11,12</sup> Pachymetric mapping technologies include slit scanning optical pachymetry<sup>13-28</sup> and very high-frequency ultrasound imaging.<sup>29,30</sup>

Pachymetric mapping provides several advantages over spot measurements. Mapping can reveal abnormal patterns such as keratoconus and pellucid marginal degeneration. It also allows preoperative planning for surgeries that primarily do not concern just the center of the cornea, such as astigmatic keratotomy, intracorneal ring segment implantation, phototherapeutic keratectomy, and lamellar keratoplasty.

Despite these advantages, conventional ultrasound spot pachymetry is still the standard because of its reliability, ease of use, and relatively low cost. The main drawback of the Orbscan slit scanning technology (Orbscan II, Bausch & Lomb, Inc., Rochester, NY) is the tendency to underestimate corneal thickness in keratoconic,<sup>21</sup> post-PRK,<sup>22-24</sup> and post-LASIK<sup>23-27</sup> eyes. In these situations, scattering from corneal haze and stromal interfaces interferes with the identification of the corneal surface reflections due to the limited resolution of slit scanning.<sup>21-23</sup> The main drawback of ultrasound imaging is the inconvenient requirement of immersing the eye in a coupling fluid. Thus, a better method of pachymetric mapping is still needed.<sup>31</sup>

Optical coherence tomography (OCT) is a noncontact cross-sectional imaging method with very high axial resolution.<sup>32,33</sup> Several investigators have used the widely available commercial retina OCT scanner (Carl Zeiss Meditec Inc., Dublin, CA) to image the cornea and measure central corneal and sublayer thicknesses.<sup>34-42</sup> Wirbelauer et al developed a slit lamp-adapted OCT system that has a larger scan width<sup>43,44</sup> and applied it to pachymetry. Neither of these systems is fast enough for pachymetric mapping because of motion artifacts in the measurements.

Advancements in OCT technology have allowed very high-speed scanning of the anterior segment of the eye at up to 4000 axial scans per second.<sup>45-47</sup> In this study, we apply the high-speed OCT technology to corneal imaging and thickness mapping. To our knowledge, this is the first article to describe pachymetric mapping with OCT.

## Materials and Methods

A high-speed corneal and anterior segment OCT prototype (Carl Zeiss Meditec) was used in the study. The prototype's performance is similar to that of the recently Food and Drug Administration-approved Zeiss Visante model. The scan rate was 2000 axial scans per second, and the optical power incident on the cornea was 5 mW. This was well below the American National Standards Institute exposure limit of 15 mW at the 1.31- $\mu$ m operating wavelength.<sup>48</sup> The axial resolution was measured to be 17  $\mu$ m full-width-half-maximum, assuming a corneal group index of 1.389.<sup>49</sup> The transverse resolution (beam diameter) was 45  $\mu$ m. The scan geometry was rectangular, with the incident OCT beam always parallel to the optical axis of the instrument. The axial scan depth was set to 4 mm. Each axial scan was sampled digitally

at 768 points, giving an axial pixel size of 5.2  $\mu\text{m}$ . The scan dimensions were calibrated with a specially designed calibration block, an aluminum plate engraved with crosshair grooves (depth = 2.493 mm) and covered with a fine metal grid mesh (30 per inch; SPI Supplies, West Chester, PA). The base plate was manufactured at the Cleveland Clinic Prototype Laboratory with a superprecise vertical machining center (SV-400, Mori Seiki Co., Nagoya, Japan) and inspected with a coordinate measuring machine (LK-CMM G-90CG, LK Metrology Systems, Inc., Brighton, MI) that has 5- $\mu\text{m}$  accuracy along the z axis. The depth of the groove on the calibration block on the OCT image was compared with the known depth to calibrate the axial pixel height. The mesh grid width on the OCT calibration image was compared with the known grid spacing to calibrate the transverse pixel width.

The corneal and anterior segment OCT scanner used a pie chart-shaped internal fixation target, and the accommodative compensation was set for the spherical equivalent refraction of each eye to optimize fixation. The scan area was visualized with a black-and-white charge-coupled device camera. The real-time charge-coupled device and OCT images were displayed simultaneously on the computer screen to facilitate scan positioning.

The cornea was mapped with 10-mm radial lines on 8 meridians centered on the vertex reflection (Fig 1A). Each meridional line consisted of 128 axial scans (a-scans) and was visualized as a cross-sectional image (Fig 2A). The entire scan pattern had 1024 a-scans and was acquired in approximately 0.5 seconds.

We developed automated computer processing for 3-dimensional corneal reconstruction and measurement. First, the anterior and posterior corneal surfaces were identified by the signal peaks at the air-tear film and cornea-aqueous interfaces on each a-scan (Fig 2B).<sup>50</sup> Then the image distortion due to refraction and transition of the group index at the air-cornea interface was removed using a dewarping algorithm.<sup>51</sup> From the dewarped image (Fig 2C), corneal thickness was measured as the distance between the anterior and posterior corneal surfaces along lines perpendicular to the anterior surface at the point of measurement. A corneal thickness profile was generated from each meridional cross section. The computer algorithm registered the 8 corneal cross sections (Fig 1B) and computed the corneal thickness (pachymetry) map by interpolation. The pachymetry map was presented on a banded color scale (Fig 3). The map was divided into a central zone (<2 mm) and 3 annular zones by diameter: pericentral, 2 to 5 mm; transitional, 5 to 7 mm; and peripheral, >7 mm. The mean, maximum, and minimum pachymetries within the central, pericentral, and transitional sectors were computed. Reproducibility was assessed by the pooled standard deviations (SDs) of the repeated measurements.

Forty-two eyes of 21 normal subjects were studied. The subjects were recruited from patients presenting in the refractive surgery department of the Cleveland Clinic Cole Eye Institute. All subjects were older than 21 years and myopic and had normal corneal topography as determined by the Atlas system (Carl Zeiss Meditec). The study protocol was approved by the institutional review board of the Cleveland Clinic Foundation. Written informed consent was obtained from all subjects. This study was in accord with Health Insurance Portability and Accountability Act of 1996 regulations. Optical coherence tomography pachymetry mapping and ultrasound central pachymetry were obtained before LASIK (all subjects) and again at the 3-month postoperative visit (13 subjects). LASIK was performed by one coauthor (DH) using an automated microkeratome (Hansatome, Bausch & Lomb, Inc., Rochester, NY) and a scanning spot excimer laser (LADARVision 4000, Alcon Laboratories, Inc., Fort Worth, TX).

Optical coherence tomography scanning was performed 3 times at each visit. The subject was asked to look at the center of the internal fixation target. The fixation target was set at 0° to align the fixation axis of the eye along the optical axis of the instrument. Rough alignment was

obtained by centering the cornea on the charge-coupled device video image. Fine alignment was adjusted using a 10-mm-long horizontal aiming scan. The operator adjusted the OCT system position to maximize the vertex reflection (Fig 2A) and placed the vertex at the center of the OCT image. Then the subject was instructed to blink and hold still while the mapping scan for 8 meridians was actuated by the operator. Subjects were repositioned after each OCT scan.

Ultrasound pachymetry was also performed 3 times at each visit by an ophthalmic technician. The 50-megahertz CorneoGage 2 (Sonogage, Cleveland, OH) was used to measure CCT after anesthetizing the cornea with 0.5% proparacaine. The 3 measurements were averaged and compared with average and minimum OCT corneal thicknesses ( $OCT_{Mean}$  and  $OCT_{Min}$ , respectively) in the central zone by linear regression, Pearson correlation, and Bland–Altman analysis.<sup>52</sup>

Post-LASIK CCT measurements (Table 1) were subtracted from preoperative readings to evaluate the amount of tissue removed during LASIK. Bland–Altman analysis was performed to compare both ultrasound measurements and OCT measurements with the ablation depth estimate given by the excimer laser system.

Image processing, thickness calculation, and Bland–Altman analysis were performed with MATLAB software (version 7.0.1, MathWorks, Inc., Natick, MA). Other statistical analyses were performed with JMP software (version 4.0.4, SAS Institute Inc., Cary, NC).

## Results

In a well-centered cross-sectional scan, the reflection from the anterior vertex of the cornea is strong enough to saturate the dynamic range of the OCT system and produce a vertical flare (Fig 2A). This phenomenon allows us to easily find the transverse location of the corneal vertex. However, where signal saturation occurs, the anterior and posterior signal peaks are broadened and the boundaries are blurred. To get around this problem, we removed the saturated axial scans from the pachymetry profiles and used a 4-knot third-order spline fitting to interpolate the missing data. The vertex area interpolated over was 0.5 to 1.0 mm in diameter. The computer-identified boundaries agreed well with our visual inspection of each dewarped cross-sectional image (Fig 2C).

A typical pachymetry map is shown in Figure 3. The thinnest area of the cornea was located slightly inferotemporal to the vertex. The cornea was thicker peripherally, as expected. For ultrasound pachymetry, the average preoperative CCT was  $553.3 \pm 33.0 \mu\text{m}$ . The  $OCT_{Mean}$  over the central zone was  $546.9 \pm 29.4 \mu\text{m}$ , and the  $OCT_{Min}$  was  $540.1 \pm 29.6 \mu\text{m}$ . Postoperatively, the ultrasound pachymetry average was  $498 \pm 46.6 \mu\text{m}$ , whereas the  $OCT_{Mean}$  was  $513.7 \pm 44.5 \mu\text{m}$  and the  $OCT_{Min}$  was  $504.4 \pm 44.9 \mu\text{m}$ .

The central OCT corneal thickness was compared with the ultrasound pachymetry readings before and after LASIK. In both situations, OCT measurements correlated very well with ultrasound pachymetry (Pearson correlation  $r = 0.97$  before surgery and  $0.98$  after LASIK; Table 2). Regression analysis of  $OCT_{Mean}$  and ultrasound data showed that the OCT measurements were slightly less than the ultrasound pachymetry before LASIK (Fig 4A) but slightly greater than the ultrasound pachymetry after LASIK (Fig 5A) [available at <http://aojournal.org>]. This was verified by the Bland–Altman analysis. Preoperatively, the difference between the  $OCT_{Mean}$  and ultrasound was  $-6.4 \mu\text{m}$  (95% limits of agreement,  $-23.2$  to  $10.4 \mu\text{m}$ ; Fig 4B). The difference between  $OCT_{Min}$  and ultrasound was  $-13.1 \mu\text{m}$  (95% limits of agreement,  $-28.8$  to  $2.5 \mu\text{m}$ ). Postoperatively, the difference between  $OCT_{Mean}$  and ultrasound was  $15.7 \mu\text{m}$  (95% limits of agreement,  $-1.6$  to  $33 \mu\text{m}$ ; Fig 5B). The postoperative difference between  $OCT_{Min}$  and ultrasound was  $6.5 \mu\text{m}$  (95% limits of agreement,  $-10$  to  $22.9$

$\mu\text{m}$ ). All differences were statistically significant ( $t$  test,  $P < 0.001$ ). Overall, the repeatability of the mean corneal thickness was roughly  $2 \mu\text{m}$  for the 3 zones within the 7-mm diameter in both pre-LASIK (Table 3) and post-LASIK (Table 4 [available at <http://aojournal.org>]) OCT pachymetry maps.

The Bland–Altman analysis showed that the tissue ablation amount measured by the OCT method agreed better (average difference,  $-5.7 \mu\text{m}$ ; 95% limits of agreement,  $-23.2$  to  $11.8 \mu\text{m}$ ) with the ablation depth estimate by the laser system than with that by the ultrasound method (average difference,  $12.1 \mu\text{m}$ ; 95% limits of agreement,  $-40.9$  to  $65.1 \mu\text{m}$ ).

## Discussion

Although focal pachymetric measurements with OCT have been described,<sup>34,37,39-42,44</sup> this article reports pachymetric mapping with OCT for the first time. Several features of the corneal and anterior segment OCT system that we demonstrated are very desirable for pachymetric mapping:

1. The high-speed OCT system acquires the pachymetric map in a short time (0.5 seconds) to reduce motion artifacts. This is faster than slit scanning technologies (2.1 seconds for Orbscan II<sup>53</sup>).
2. Optical coherence tomography has a high axial resolution, allowing the corneal boundaries to be clearly defined by distinct signal peaks, free of interference from stromal reflections. In contrast, slit scanning technology has much lower axial resolution, and corneal edge detection can be confounded by subepithelial haze and other stromal reflections.<sup>53</sup>
3. Unlike ultrasound, the measurement does not require contact or immersion.
4. The accommodation-adjusted fixation target optimizes the establishment of the fixation axis.
5. The rectangular scan geometry, in addition to the fixation target, provides an accurate corneal vertex landmark.

In our study, the OCT central pachymetry was slightly thinner than standard ultrasound pachymetry before LASIK surgery, but slightly thicker postoperatively. The measurement difference was  $-6.4 \pm 8.6 \mu\text{m}$  before surgery and  $15.7 \pm 8.8 \mu\text{m}$  after surgery. The 95% limits of agreement in both cases, as Bland and Altman<sup>52</sup> suggested, have a span of approximately  $30 \mu\text{m}$ . This difference is statistically significant, but no more than the CCT difference measured with different ultrasound pachymeters. Reader and Salz reported a maximum difference of  $49 \mu\text{m}$  on CCT measurement with different ultrasound pachymeters.<sup>54</sup> Miranda et al observed a significant LASIK flap thickness variation of  $21$  to  $40 \mu\text{m}$  in SD, depending on the microkeratome and setting.<sup>55</sup> The average CCT of normal eyes is  $536 \pm 31 \mu\text{m}$  (median  $\pm$  SD), as determined by a meta-analysis.<sup>56</sup> These variations are much larger than the small difference between OCT and ultrasound pachymetry described in this study. Based on these comparisons, the differences between OCT and ultrasound central pachymetry are relatively small, and they could be used interchangeably both before and after a LASIK procedure.

There are several theoretical explanations for the small systematic difference between OCT and ultrasound pachymetry measurements in our current study. The OCT measurement includes the tear film, whereas the ultrasound contact probe displaces the tear film. This could bias the OCT measurement slightly toward a higher value. Our OCT methodology should provide better measurement centration and perpendicularity than ultrasound pachymetry. This could bias the OCT measurement slightly toward a lower value. Post–myopic LASIK central corneal epithelial thickening<sup>57-60</sup> and shifts in stromal hydration<sup>61,62</sup> could alter the corneal

index and acoustic velocity, which in turn affects OCT and ultrasound thickness measurements. In addition, there could be small calibration errors for either system. The excellent agreement we obtained between OCT and ultrasound suggests that these errors are small.

Previous OCT studies<sup>39,40,63</sup> showed that OCT pachymetry correlated well with ultrasound but tended toward underestimation (mean difference: Bechmann et al, 49.4  $\mu\text{m}$ ; Wong et al, 32  $\mu\text{m}$ ; Wirbelauer et al, 23  $\mu\text{m}$ ). The difference is much smaller in our study. One possible explanation is that we averaged the OCT pachymetry over the central 2 mm rather than using a single focal measurement. There also may have been differences in calibration.

We were not able to compare our OCT pachymetry measurements in off-center sectors with a reference technology because we did not have access to an alternative pachymetric mapping system. We are conducting a comparative study with the Orbscan II, and we hope others will be able to conduct comparative studies with other pachymetric mapping systems such as the Artemis (very high-frequency ultrasound; Ultralink, St. Petersburg, FL) and Pentacam (Scheimpflug photography; Oculus, Inc., Dutenhofen, Germany). Based on our data, pachymetry measurement in the sectors up to 7 mm diameter is highly reproducible. Because the anterior and posterior boundary peaks are clearly identifiable, we believe these measurements should be as accurate as the central measurement. However, signals from the peripheral zone (>7-mm diameter) are weaker, and the thickness measurement is not as reliable. Another limitation of the current OCT technology is that interpolation is used in the central 0.5- to 1.0-mm diameter and among the 8 radial scans. Thus, small areas of corneal thickness variation might be missed.

In summary, for the first time we have demonstrated reproducible pachymetric mapping over a wide area of the cornea using a high-speed corneal and anterior segment OCT system. This technology could be valuable for the planning of keratorefractive procedures and diagnosis of corneal diseases.

## References

1. Waring GO III, Bourne WM, Edelhauser HF, Kenyon KR. The corneal endothelium. Normal and pathologic structure and function. *Ophthalmology* 1982;89:531–90. [PubMed: 7122038]
2. O'Neal MR, Polse KA. In vivo assessment of mechanisms controlling corneal hydration. *Invest Ophthalmol Vis Sci* 1985;26:849–56. [PubMed: 4008195]
3. Cheng H, Bates AK, Wood L, McPherson K. Positive correlation of corneal thickness and endothelial cell loss. Serial measurements after cataract surgery. *Arch Ophthalmol* 1988;106:920–2. [PubMed: 3390055]
4. Holden BA, Mertz GW, McNally JJ. Corneal swelling response to contact lenses worn under extended wear conditions. *Invest Ophthalmol Vis Sci* 1983;24:218–26. [PubMed: 6826325]
5. Copt RP, Thomas R, Mermoud A. Corneal thickness in ocular hypertension, primary open-angle glaucoma, and normal tension glaucoma. *Arch Ophthalmol* 1999;117:14–6. [PubMed: 9930155]
6. Brandt JD, Beiser JA, Gordon MO, et al. Central corneal thickness and measured IOP response to topical ocular hypotensive medication in the Ocular Hypertension Treatment Study. *Am J Ophthalmol* 2004;138:717–22. [PubMed: 15531304]
7. Nissen J, Hjortdal JO, Ehlers N, et al. A clinical comparison of optical and ultrasonic pachometry. *Acta Ophthalmol (Copenh)* 1991;69:659–63. [PubMed: 1776423]
8. McLaren JW, Nau CB, Erie JC, Bourne WM. Corneal thickness measurement by confocal microscopy, ultrasound, and scanning slit methods. *Am J Ophthalmol* 2004;137:1011–20. [PubMed: 15183784]
9. Kozak I, Hornak M, Juhas T, et al. Changes in central corneal thickness after laser in situ keratomileusis and photorefractive keratectomy. *J Refract Surg* 2003;19:149–53. [PubMed: 12701720]
10. Rabinowitz YS, Rasheed K, Yang H, Elashoff J. Accuracy of ultrasonic pachymetry and videokeratography in detecting keratoconus. *J Cataract Refract Surg* 1998;24:196–201. [PubMed: 9530594]

11. Huang D, Wang J, Lin CP, et al. Micron-resolution ranging of cornea anterior chamber by optical reflectometry. *Lasers Surg Med* 1991;11:419–25. [PubMed: 1816476]
12. Böhnke M, Masters BR, Wälti R, et al. Precision and reproducibility of measurements of human corneal thickness with rapid optical low-coherence reflectometry (OLCR). *J Biomed Opt* 1999;4:152–6.
13. Modis L Jr, Langenbucher A, Seitz B. Evaluation of normal corneas using the scanning-slit topography/pachymetry system. *Cornea* 2004;23:689–94. [PubMed: 15448494]
14. Suzuki S, Oshika T, Oki K, et al. Corneal thickness measurements: scanning-slit corneal topography and noncontact specular microscopy versus ultrasonic pachymetry. *J Cataract Refract Surg* 2003;29:1313–8. [PubMed: 12900238]
15. Yaylali V, Kaufman SC, Thompson HW. Corneal thickness measurements with the Orbscan Topography System and ultrasonic pachymetry. *J Cataract Refract Surg* 1997;23:1345–50. [PubMed: 9423906]
16. Radford SW, Lim R, Salmon JF. Comparison of Orbscan and ultrasound pachymetry in the measurement of central corneal thickness [letter]. *Eye* 2004;18:434–6. [PubMed: 15069445]
17. Gonzalez-Mejome JM, Cervino A, Yebra-Pimentel E, Parafita MA. Central and peripheral corneal thickness measurement with Orbscan II and topographical ultrasound pachymetry. *J Cataract Refract Surg* 2003;29:125–32. [PubMed: 12551679]
18. Rainer G, Findl O, Petternel V, et al. Central corneal thickness measurements with partial coherence interferometry, ultrasound, and the Orbscan system. *Ophthalmology* 2004;111:875–9. [PubMed: 15121362]
19. Liu Z, Huang AJ, Pflugfelder SC. Evaluation of corneal thickness and topography in normal eyes using the Orbscan corneal topography system. *Br J Ophthalmol* 1999;83:774–8. [PubMed: 10381661]
20. Auffarth GU, Wang L, Volcker HE. Keratoconus evaluation using the Orbscan Topography System. *J Cataract Refract Surg* 2000;26:222–8. [PubMed: 10683789]
21. Gherghel D, Hosking SL, Mantry S, et al. Corneal pachymetry in normal and keratoconic eyes: Orbscan II versus ultrasound. *J Cataract Refract Surg* 2004;30:1272–7. [PubMed: 15177603]
22. Boscia F, La Tegola MG, Alessio G, Sborgia C. Accuracy of Orbscan optical pachymetry in corneas with haze. *J Cataract Refract Surg* 2002;28:253–8. [PubMed: 11821206]
23. Prisant O, Calderon N, Chastang P, et al. Reliability of pachymetric measurements using Orbscan after excimer refractive surgery. *Ophthalmology* 2003;110:511–5. [PubMed: 12623813]
24. Fakhry MA, Artola A, Belda JI, et al. Comparison of corneal pachymetry using ultrasound and Orbscan II. *J Cataract Refract Surg* 2002;28:248–52. [PubMed: 11821205]
25. Iskander NG, Anderson Penno E, Peters NT, et al. Accuracy of Orbscan pachymetry measurements and DHG ultrasound pachymetry in primary laser in situ keratomileusis and LASIK enhancement procedures. *J Cataract Refract Surg* 2001;27:681–5. [PubMed: 11377895]
26. Kawana K, Tokunaga T, Miyata K, et al. Comparison of corneal thickness measurements using Orbscan II, non-contact specular microscopy, and ultrasonic pachymetry in eyes after laser in situ keratomileusis. *Br J Ophthalmol* 2004;88:466–8. [PubMed: 15031156]
27. Chakrabarti HS, Craig JP, Brahma A, et al. Comparison of corneal thickness measurements using ultrasound and Orbscan slit-scanning topography in normal and post-LASIK eyes. *J Cataract Refract Surg* 2001;27:1823–8. [PubMed: 11709257]
28. Rufer F, Schroder A, Arvani M, Erb C. Central and peripheral corneal pachymetry—standard evaluation with the Pentacam system [in German]. *Klin Monatsbl Augenheilkd* 2005;222:117–22. [PubMed: 15719315]
29. Reinstein DZ, Silverman RH, Raevsky T, et al. Arc-scanning very high-frequency digital ultrasound for 3D pachymetric mapping of the corneal epithelium and stroma in laser in situ keratomileusis. *J Refract Surg* 2000;16:414–30. [PubMed: 10939721]
30. Reinstein DZ, Silverman RH, Trokel SL, Coleman DJ. Corneal pachymetric topography. *Ophthalmology* 1994;101:432–8. [PubMed: 8127563]
31. Huang D. A reliable corneal tomography system is still needed. *Ophthalmology* 2003;110:455–6. [PubMed: 12623804]

32. Huang D, Swanson EA, Lin CP, et al. Optical coherence tomography. *Science* 1991;254:1178–81. [PubMed: 1957169]
33. Izatt JA, Hee MR, Swanson EA, et al. Micrometer-scale resolution imaging of the anterior eye in vivo with optical coherence tomography. *Arch Ophthalmol* 1994;112:1584–9. [PubMed: 7993214]
34. Maldonado MJ, Ruiz-Oblitas L, Munuera JM, et al. Optical coherence tomography evaluation of the corneal cap and stromal bed features after laser in situ keratomileusis for high myopia and astigmatism. *Ophthalmology* 2000;107:81–7. [PubMed: 10647724]discussion 88
35. Ustundag C, Bahcecioglu H, Ozdamar A, et al. Optical coherence tomography for evaluation of anatomical changes in the cornea after laser in situ keratomileusis. *J Cataract Refract Surg* 2000;26:1458–62. [PubMed: 11033391]
36. Hirano K, Ito Y, Suzuki T, et al. Optical coherence tomography for the noninvasive evaluation of the cornea. *Cornea* 2001;20:281–9. [PubMed: 11322417]
37. Muscat S, McKay N, Parks S, et al. Repeatability and reproducibility of corneal thickness measurements by optical coherence tomography. *Invest Ophthalmol Vis Sci* 2002;43:1791–5. [PubMed: 12036980]
38. Wang J, Fonn D, Simpson TL, Jones L. Relation between optical coherence tomography and optical pachymetry measurements of corneal swelling induced by hypoxia. *Am J Ophthalmol* 2002;134:93–8. [PubMed: 12095814]
39. Bechmann M, Thiel MJ, Neubauer AS, et al. Central corneal thickness measurement with a retinal optical coherence tomography device versus standard ultrasonic pachymetry. *Cornea* 2001;20:50–4. [PubMed: 11189004]
40. Wong AC, Wong CC, Yuen NS, Hui SP. Correlational study of central corneal thickness measurements on Hong Kong Chinese using optical coherence tomography, Orbscan and ultrasound pachymetry. *Eye* 2002;16:715–21. [PubMed: 12439665]
41. Feng Y, Varikooty J, Simpson TL. Diurnal variation of corneal and corneal epithelial thickness measured using optical coherence tomography. *Cornea* 2001;20:480–3. [PubMed: 11413402]
42. Fishman GR, Pons ME, Seedor JA, et al. Assessment of central corneal thickness using optical coherence tomography. *J Cataract Refract Surg* 2005;31:707–11. [PubMed: 15899446]
43. Wirbelauer C, Pham DT. Monitoring corneal structures with slitlamp-adapted optical coherence tomography in laser in situ keratomileusis. *J Cataract Refract Surg* 2004;30:1851–60. [PubMed: 15342046]
44. Wirbelauer C, Scholz C, Hoerauf H, et al. Noncontact corneal pachymetry with slit lamp-adapted optical coherence tomography. *Am J Ophthalmol* 2002;133:444–50. [PubMed: 11931776]
45. Radhakrishnan S, Rollins AM, Roth JE, et al. Real-time optical coherence tomography of the anterior segment at 1310 nm. *Arch Ophthalmol* 2001;119:1179–85. [PubMed: 11483086]
46. Huang, D.; Li, Y.; Radhakrishnan, S.; Chalita, MR. Corneal and anterior segment optical coherence tomography. In: Schuman, JS.; Puliafito, CA.; Fujimoto, JG., editors. *Optical Coherence Tomography of Ocular Diseases*. 2nd ed.. SLACK Inc.; Thorofare, NJ: 2004. p. 663-73.
47. Goldsmith JA, Li Y, Chalita MR, et al. Anterior chamber width measurement by high-speed optical coherence tomography. *Ophthalmology* 2005;112:238–44. [PubMed: 15691557]
48. Laser Institute of America; Orlando: 2000. American National Standard for Safe Use of Lasers. ANSI Z136.1-2000; p. 45
49. Lin R, Shure M, Rollins A, et al. Group index of the human cornea at 1.3-micron wavelength obtained in vitro by optical coherence domain reflectometry. *Opt Lett* 2004;29:83–5. [PubMed: 14719668]
50. Li Y, Shekhar R, Huang D, Sonka M, Fitzpatrick JM. Segmentation of 830- and 1310-nm LASIK corneal optical coherence tomography images. *Medical Imaging 2002: Image Processing. Proceedings of SPIE* 2002;4684:167–78.
51. Westphal V, Rollins AM, Radhakrishnan S, Izatt JA. Correction of geometric and refractive image distortions in optical coherence tomography applying Fermat's principle. *Opt Express* [serial online] 2002;10:397–404. <http://www.opticsexpress.org/abstract.cfm?URI=OPEX-10-9-397> Available at Accessed January 30, 2006
52. Bland JM, Altman DG. Measuring agreement in method comparison studies. *Stat Methods Med Res* 1999;8:135–60. [PubMed: 10501650]



53. Cairns G, McGhee CN. Orbscan computerized topography: attributes, applications, and limitations. *J Cataract Refract Surg* 2005;31:205–20. [PubMed: 15721715]
54. Reader AL III, Salz JJ. Differences among ultrasonic pachymeters in measuring corneal thickness. *J Refract Surg* 1987;3:7–11.
55. Miranda D, Smith SD, Krueger RR. Comparison of flap thickness reproducibility using microkeratomes with a second motor for advancement. *Ophthalmology* 2003;110:1931–4. [PubMed: 14522767]
56. Doughty MJ, Zaman ML. Human corneal thickness and its impact on intraocular pressure measures: a review and meta-analysis approach. *Surv Ophthalmol* 2000;44:367–408. [PubMed: 10734239]
57. Reinstein DZ, Silverman RH, Sutton HF, Coleman DJ. Very high-frequency ultrasound corneal analysis identifies anatomic correlates of optical complications of lamellar refractive surgery: anatomic diagnosis in lamellar surgery. *Ophthalmology* 1999;106:474–82. [PubMed: 10080202]
58. Dawson DG, Holley GP, Geroski DH, et al. Ex vivo confocal microscopy of human LASIK corneas with histologic and ultrastructural correlation. *Ophthalmology* 2005;112:634–44. [PubMed: 15808255]
59. Dawson DG, Edelhauser HF, Grossniklaus HE. Long-term histopathologic findings in human corneal wounds after refractive surgical procedures. *Am J Ophthalmol* 2005;139:168–78. [PubMed: 15652843]
60. Lohmann CP, Guell JL. Regression after LASIK for the treatment of myopia: the role of the corneal epithelium. *Semin Ophthalmol* 1998;13:79–82. [PubMed: 9758652]
61. Grzybowski DM, Roberts CJ, Mahmoud AM, Chang JS Jr. Model for nonectatic increase in posterior corneal elevation after ablative procedures. *J Cataract Refract Surg* 2005;31:72–81. [PubMed: 15721698]
62. Potgieter FJ, Roberts C, Cox IG, et al. Prediction of flap response. *J Cataract Refract Surg* 2005;31:106–14. [PubMed: 15721702]
63. Wirbelauer C, Scholz C, Hoerauf H, et al. Corneal optical coherence tomography before and immediately after excimer laser photorefractive keratectomy. *Am J Ophthalmol* 2000;130:693–9. [PubMed: 11124285]

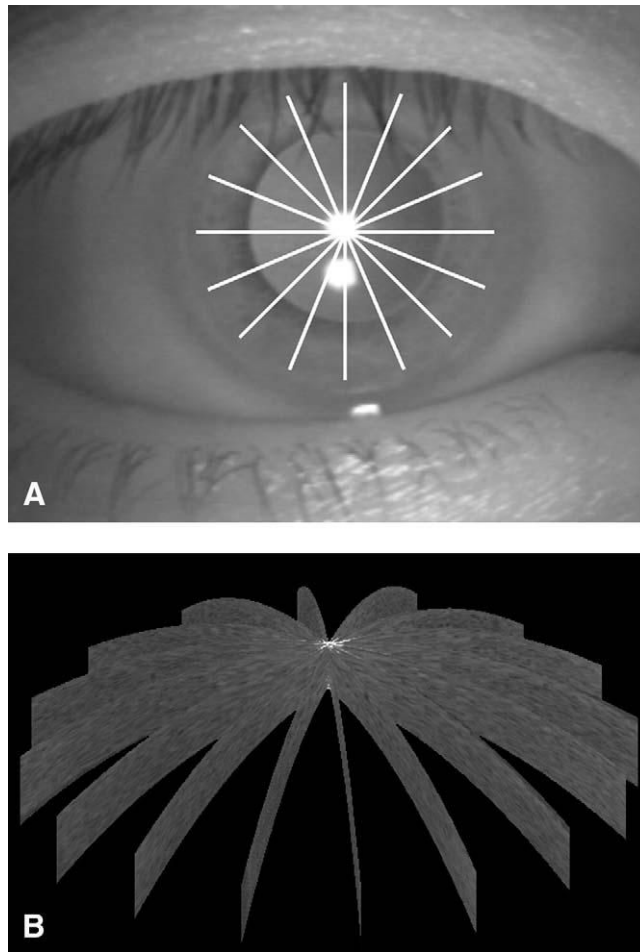


**Figure 1.**

**A,** Optical coherence tomography scan pattern for pachymetry mapping shown on a frame of charge-coupled device video image. The pattern consisted of 8 radial lines of 10-mm length.

**B,** Three-dimensional reconstruction of the cornea from 8 dewarped cross sections.

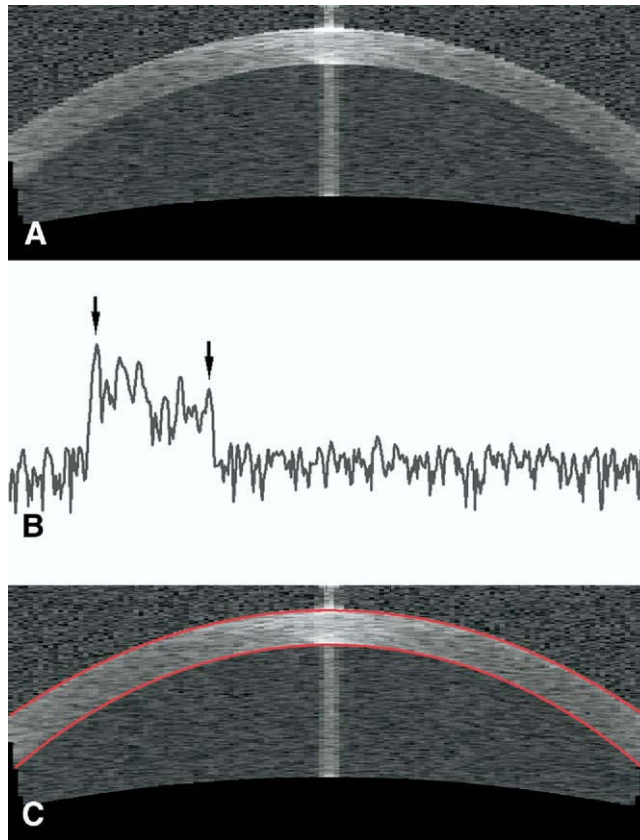


**Figure 2.**  
**A,** Cross-sectional optical coherence tomography (OCT) image from 1 of the 8 radial line scans. **B,** An OCT axial scan from pericentral cornea plotted on a logarithmic scale. Arrows mark the signal peaks at the anterior (left) and posterior (right) corneal boundaries located by the automated algorithm. **C,** Dewarped OCT cross section overlaid with detected corneal boundaries.

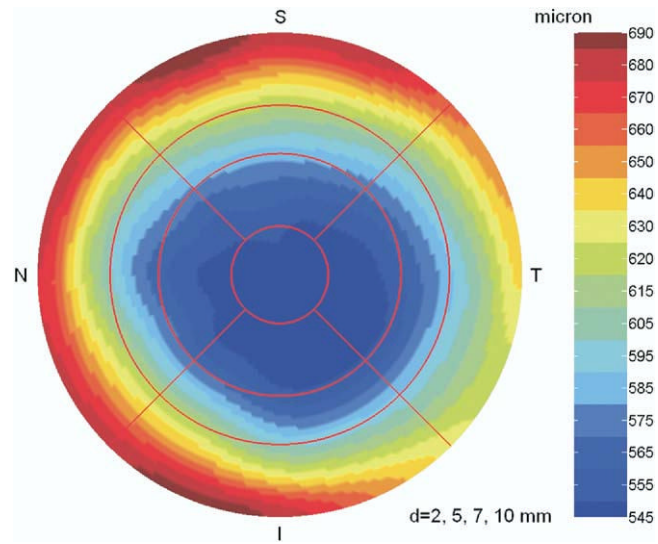


**Figure 3.** A corneal pachymetry map. d = diameter; I = inferior; N = nasal; S = superior; T = temporal.



**Figure 4.** Pre-LASIK optical coherence tomography (OCT) central corneal thickness compared with the ultrasound (US) pachymetry measurement.  $OCT_{Mean}$  = average OCT corneal thickness over the central zone. **A**, Regression analysis.  $y = x$  is the line of equality. The 95% confidence interval (CI) of the slope was 0.789 to 0.936. The 95% CI of the y intercept was 29 to 110.1  $\mu\text{m}$ . The  $R^2$  of the fit was 0.939. **B**, Bland–Altman plot. The distribution of the mean (x axis) and the difference (y axis) between US pachymetry and OCT reflects the level of agreement. The mean difference was  $-6.4 \mu\text{m}$ , with 95% limits of agreement from  $-23.2$  to  $10.4 \mu\text{m}$ . SD = standard deviation.

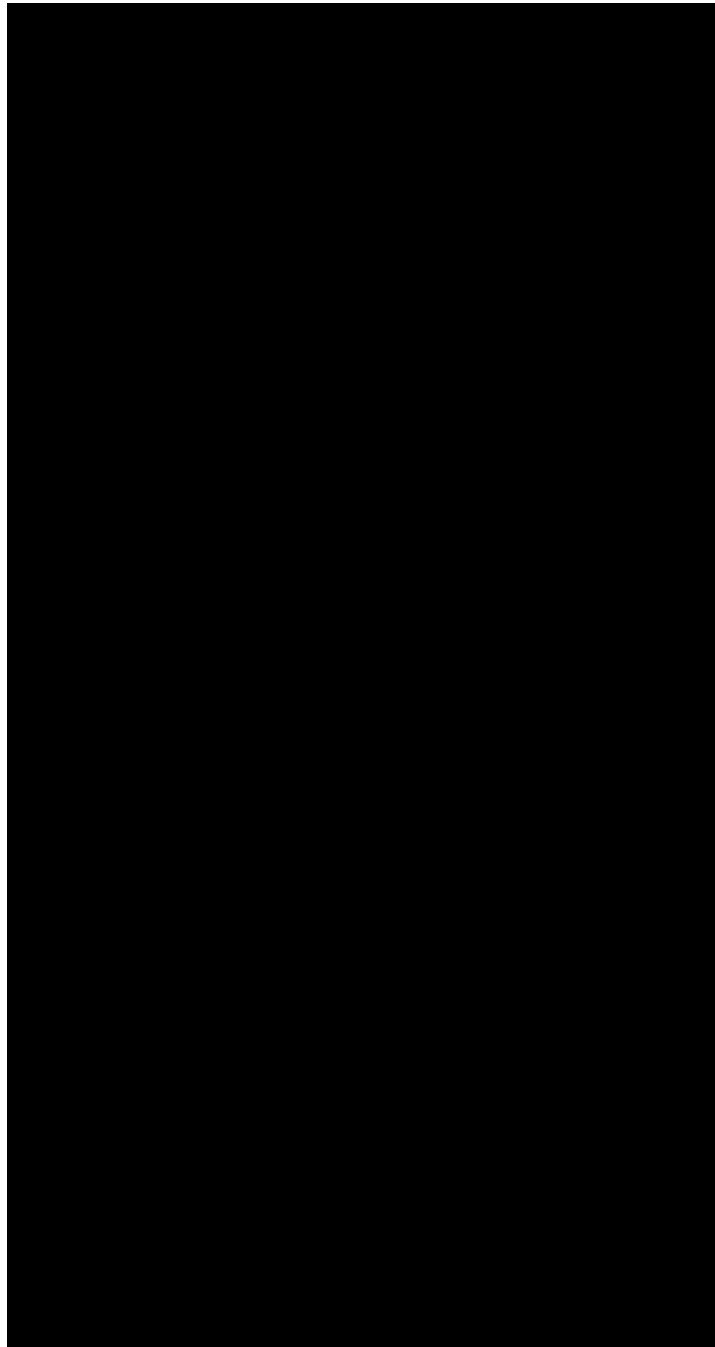


**Figure 5.** Post-LASIK optical coherence tomography (OCT) central corneal thickness compared with the ultrasound (US) pachymetry measurement.  $OCT_{Mean}$  = average OCT corneal thickness over the central zone. **A**, Regression analysis plot.  $y = x$  is the line of equality. The 95% confidence interval (CI) of the slope was 0.862 to 1.018. The 95% CI of the y intercept was 6.7 to 84.3  $\mu\text{m}$ . The  $R^2$  of the fit was 0.964. **B**, Bland–Altman plot. The distribution of the mean (x axis) and the difference (y axis) between US pachymetry and OCT reflects the level of agreement. The mean difference was 15.7  $\mu\text{m}$ , with 95% limits of agreement from  $-1.6$  to 33  $\mu\text{m}$ . SD = standard deviation.

**Table 1**

## Central Corneal Thickness Measurements

	Pre-LASIK		Post-LASIK	
	<i>Mean ± SD (μm)</i>	<i>Range (μm)</i>	<i>Mean ± SD (μm)</i>	<i>Range (μm)</i>
US	553.3±33.0	489–607	498±46.6	405–574
OCT <sub>Mean</sub>	546.9±29.4	477–599	513.7±44.5	437–587
OCT <sub>Min</sub>	540.1±29.6	471–584	504.4±44.9	424–580

OCT = optical coherence tomography; OCT<sub>Mean</sub> = average OCT corneal thickness over the central zone (diameter < 2 mm); OCT<sub>Min</sub> = minimum OCT corneal thickness over the central zone; SD = standard deviation; US = ultrasound pachymetry.

**Table 2**  
Optical Coherence Tomography Pachymetry Measurements Compared with Ultrasound Pachymetry Measurements

	Mean Difference ( $\mu\text{m}$ )	95% Limits of Agreement ( $\mu\text{m}$ )	Correlation ( $r$ )
Pre-LASIK			
OCT <sub>Mean</sub> – US	$-6.4 \pm 8.6$	-23.2 to 10.4	0.969
OCT <sub>Min</sub> – US	$-13.1 \pm 8.0$	-28.8 to 2.5	0.973
Post-LASIK			
OCT <sub>Mean</sub> – US	$15.7 \pm 8.8$	-1.6 to 33	0.982
OCT <sub>Min</sub> – US	$6.5 \pm 8.4$	-10.0 to 22.9	0.984

OCT = optical coherence tomography; OCT<sub>Mean</sub> = average OCT corneal thickness over the central zone; OCT<sub>Min</sub> = minimum OCT corneal thickness over the central zone; US = ultrasound pachymetry.



**Table 3**  
Pre-LASIK Optical Coherence Tomography Pachymetry Map Zonal Repeatability by Pooled Standard Deviations

	Maximum ( $\mu\text{m}$ )	Minimum ( $\mu\text{m}$ )	Average ( $\mu\text{m}$ )
Central (D < 2 mm)	2.3	2.1	1.6
Pericentral (D = 2–5 mm)	4.8	2.3	1.5
Transitional (D = 5–7 mm)	8.1	4.0	2.4

D = diameter.

**Table 4**  
Post-LASIK Optical Coherence Tomography Pachymetry Zonal Repeatability by Pooled Standard Deviation

	Maximum ( $\mu\text{m}$ )	Minimum ( $\mu\text{m}$ )	Average ( $\mu\text{m}$ )
Central (D < 2 mm)	2.9	2.1	1.7
Pericentral (D = 2–5 mm)	5.0	2.3	1.6
Transitional (D = 5–7 mm)	8.2	4.5	2.3
D = diameter.			